Am J Physiol Heart Circ Physiol 307: H1469–H1477, 2014.
First published September 19, 2014; doi:10.1152/ajpheart.00553.2014.

Cardiac P2X purinergic receptors as a new pathway for increasing Na^+ entry in cardiac myocytes

Jian-Bing Shen,* Ronghua Yang,* Achilles Pappano, and Bruce T. Liang

Pat and Jim Calhoun Cardiology Center, University of Connecticut Medical Center, Farmington, Connecticut

Submitted 7 August 2014; accepted in final form 16 September 2014

Shen JB, Yang R, Pappano A, Liang BT. Cardiac P2X purinergic receptors as a new pathway for increasing Na^+ entry in cardiac myocytes. *Am J Physiol Heart Circ Physiol* 307: H1469–H1477, 2014. First published September 19, 2014; doi:10.1152/ajpheart.00553.2014.—P2X4 receptors (P2X4Rs) are ligand-gated ion channels capable of conducting cations such as Na^+. Endogenous cardiac P2X4R can mediate ATP-activated current in adult murine cardiomyocytes. In the present study, we tested the hypothesis that cardiac P2X receptors can induce Na^+ entry and modulate Na^+ handling. We further determined whether P2X receptor-induced stimulation of the Na^+/Ca^{2+} exchanger (NCX) has a role in modulating the cardiac contractile state. Changes in Na^+-K^+-ATPase current (I_p) and NCX current (I_{NCX}) after agonist stimulation were measured in ventricular myocytes of P2X4 transgenic mice using whole cell patch-clamp techniques. The agonist 2-methylthio-ATP (2-meSATP) increased peak I_p from a basal level of 0.52 ± 0.02 to 0.58 ± 0.03 pA/pF. 2-meSATP also increased the Ca^{2+} entry mode of I_{NCX} (0.55 ± 0.09 pA/pF under control conditions vs. 0.82 ± 0.14 pA/pF with 2-meSATP) at a membrane potential of +50 mV. 2-meSATP shifted the reversal potential of I_{NCX} from −14 ± 2.3 to −25 ± 4.1 mV, causing an estimated intracellular Na^+ concentration increase of 1.28 ± 0.42 mM. These experimental results were closely mimicked by mathematical simulations based on previously established models. KB-R7943 or a structurally different agent preferentially opposing the Ca^{2+} entry mode of NCX, YM-244769, could inhibit the 2-meSATP-induced increase in cell shortening in transgenic myocytes. Thus, the Ca^{2+} entry mode of I_{NCX} participates in P2X agonist-stimulated contractions. In ventricular myocytes from wild-type mice, the P2X agonist could increase I_{NCX}, and KB-R7943 was able to inhibit the contractile effect of endogenous P2X4Rs, indicating a physiological role of these receptors in wild-type cells. The data demonstrate a novel Na^+ entry pathway through ligand-gated P2X4Rs in cardiomyocytes.

purinergic receptors; Na^+-K^+-ATPase; Na^+/Ca^{2+} exchanger; contraction; myocytes

INTRACELLULAR Na^+ CONCENTRATION ($[Na^+]_i$) and its homeostasis are important in regulating the contractile and electrical activity of the heart (2). Sarcolemmal Na^+-K^+-ATPase (Na^+ pump), with energy derived from the hydrolysis of ATP, generates an outward pump current carried by Na^+ at rest as well as during action potentials (6). The Na^+/Ca^{2+} exchanger (NCX), through its Ca^{2+} entry mode, can also extrude Na^+ from the cardiac myocyte (7, 11). Several members of both P2X receptor (P2XR) and P2Y receptor subfamilies, including P2X4 receptors (P2X4Rs), are expressed in the heart (1, 16). Activation of cardiac P2XRs by extracellular ATP enhances the contraction of isolated myocytes and intact hearts (15, 20). Cardiac-specific transgenic (TG) overexpression of human P2X4Rs (P2X4R TG) enhanced basal and 2-methylthio-ATP (2-meSATP)-stimulated contractions (8). Overexpression of the P2X4R protected against calsequestrin overexpression-induced pressure overload and postinfarct heart failure (30, 35, 36, 37). A physiological role of endogenous cardiac myocyte P2X4Rs was recently studied (37). Using cardiac-specific conditional knockout of P2X4Rs, the study showed that knockout mice exhibited a more severe heart failure phenotype after left coronary ligation and after aortic banding.

P2XRs are ligand-gated ion channels that are permeable to Na^+, K^+, and Ca^{2+} with a reversal potential near 0 mV (17, 22). Extracellular ATP can induce nonselective cationic current in murine (27), rat (25), and guinea pig (19) cardiac ventricular myocytes. Under normal extracellular Ca^{2+} concentration ($[Ca^{2+}]_o$; 1.8 mM), Ca^{2+} contributes ~8% of the total inward current induced by ATP via homotrimeric human P2X4Rs expressed in human embryonic kidney cells (4). However, most of the ATP-induced inward current is carried by Na^+ (4, 27). In the present study, we examined the effects of Na^+ entry via P2XRs on the activities of either the Na^+ pump or NCX as each is sensitive to intracellular Na^+ changes. Myocyte contraction was also tested in the presence of Ca^{2+} entry mode NCX inhibitors KB-R7943 (2-{2-[4-(4-nitrobenzyloxyl)phenyl]ethyl}isothiourea) or YM-244769 (9*N*-(3-aminobenzyl)-6-{4-[(3-fluorobenzyl)oxyl]phenoxy} nicotinamide) to determine the role of NCX in 2-meSATP-stimulated contraction. Experiments were carried out in P2X4R TG cardiac ventricular myocytes to facilitate detection of an effect on Na^+ pump and NCX activities by P2X agonist. Current-voltage (*I–V*) relationships of the Na^+ pump and NCX were also simulated with mathematical modeling (14). Similar experiments were carried out in ventricular myocytes from wild-type (WT) mice to explore the physiological relevance of this receptor in modulating Na^+ handling.

MATERIALS AND METHODS

Isolation of adult cardiac ventricular myocytes. P2X4R TG mice were generated and bred as previously described (9, 27, 35). Animals were maintained according to a protocol approved by the Institutional Animal Care and Use Committee of the University of Connecticut Health Center and conformed with the National Institutes of Health *Guide for the Care and Use of Laboratory Animals*. Cardiac ventricular myocytes were obtained from 3-mo-old P2X4 TG or WT mice of either sex by an enzymatic dissociation procedure (27). Briefly, we cannulated the aorta of excised hearts and perfused it at 37°C with Ca^{2+}-free oxygenated buffer containing (in mM) 125 NaCl, 4.4 KCl, 1 $MgCl_2$, 4 HEPES, 18 $NaHCO_3$, 11 glucose, and 3 2,3-butanedione monoxime (pH 7.3). After 2–3 min, the coronaries were free of blood, and the perfusion buffer was switched to the same buffer containing 0.08 mg/ml Liberase Blendzyme 4 (Roche Molecular Biochemicals) and 25 μM $CaCl_2$ for 10 min. The left ventricles were minced and titurated to yield myocytes. Myocytes were then exposed ultimately to

* J.-B. Shen and R. Yang contributed equally to this work.

Address for reprint requests and other correspondence: B. Liang, Pat and Jim Calhoun Cardiology Center, Univ. of Connecticut School of Medicine, 263 Farmington Ave., MC3946, Farmington, CT 06032 (e-mail: bliang@uchc.edu).

and kept at 1.0 mM external $CaCl_2$ for experiments. At the end of the isolation procedure, myocytes that were studied needed to meet the criteria of maintaining a rod shape without blebs or blurred striation in light microscopy, remaining quiescent without spontaneous contraction, and capable of being paced for contraction shortening measurements. All myocytes were studied without any preselection bias. Experiments were carried out at room temperature (22–23°C) and were completed within 5 h after myocyte isolation.

Whole cell patch-clamp method. Electrodes were prepared from borosilicate glass pipette (1.2-mm inner diameter) with a two-step pulling procedure and filled with pipette solution (see below). Electrode resistances were 2–4 MΩ. The pipette was connected via an Ag-AgCl wire to the head stage of an amplifier (List EPC-7, Medical Systems, Greenvale, NY). After electrical contact was established for a few minutes, membrane capacitance was calculated from a −5-mV voltage step. Voltage commands and data acquisition were accomplished with Axon pCLAMP software (version 9.0).

NCX current measurement. To measure NCX current (I_{NCX}), electrodes were filled with a solution containing (mM) 135 cesium aspartate, 5 Na_2ATP, 3 $MgCl_2$, 10 HEPES, and 10 EGTA (pH 7.3 adjusted with CsOH). The outlet of a rapid solution changing device (SF-77B, Warner Instrument) was brought within 50 μm of the cell. The superfusion medium was then changed to a modified Tyrode solution (5.4 mM KCl was omitted and 10 mM CsCl, 10 μM nifedipine, and 5 μM ouabain were added to Tyrode solution) to block K^+ current, L-type Ca^{2+} current ($I_{Ca,L}$), and Na^+ pump current (I_p), respectively. The voltage protocol used to elicit I_{NCX} was as follows: from a holding potential of −80 mV, a brief 10-ms step to +80 mV was followed by a 2-s repolarizing ramp to −100 mV. The ramp was applied to myocytes three times at 1-s intervals, and the superfusing fluid was then rapidly changed to a solution containing 10 mM $NiCl_2$ for 10 s. At the end of the Ni^{2+} application, the same ramp protocol was applied again. Three Ni^{2+}-sensitive current traces from 60 to 100 mV were averaged to construct the *I–V* relationship of I_{NCX} under control conditions (5, 34). 2-meSATP (3 μM) was then added to the superfusion solution for 3–4 min while the myocyte was clamped at −80 mV. The same procedures of ramp protocol and rapid solution change were applied again in the presence of 2-meSATP. The *I–V* relationship of I_{NCX}, taken as the Ni^{2+}-sensitive current, was compared in the absence and presence of 2-meSATP.

To measure only the Ca^{2+} entry mode of I_{NCX}, the current at +30 mV was continuously recorded before and after rapid application of 10 mM Ni^{2+}. During the subsequent 2-meSATP exposure, the myocyte was held at −80 mV to promote Na^+ entry. After 3–4 min, the holding potential was changed to +30 mV again, and Ni^{2+} was applied to block the Ca^{2+} entry mode of I_{NCX}.

I_p measurement. Myocytes were voltage clamped with the same pipette solution as in I_{NCX} experiments. Pipette Na^+ was varied from 5 to 100 mM by equimolar adjustment of Cs^+ and Na^+ concentrations. After electrical contact was established and membrane capacitance was obtained, the bath solution was then changed to 0 mM K^+-containing Tyrode solution to block I_p. The solution also contained 5 mM $NiCl_2$ to block I_{NCX} and $I_{Ca,L}$ (31, 33). The holding potential was set to −80 mV to promote 2-meSATP-induced inward current. I_p was measured as K^+-activated outward current elicited by rapidly changing the extracellular solution from 0 mM K^+- to 5.4 mM K^+-modified Tyrode solution for 5 s. The holding potential was switched to −20 mV to obtain the maximal activation of I_p. Peak I_p was selected to evaluate Na^+-K^+-ATPase activity before and after 2-meSATP application, since the Na^+ changes sensed by Na^+-K^+-ATPase are more accurately reflected by peak I_p than steady I_p (31). The brief exposure to K^+ containing extracellular solution minimized the change of the intracellular ion environment during 2-meSATP application. After peak I_p was obtained under control conditions, 3 μM 2-meSATP was added to the superfusion solution for 3–4 min while the myocyte was clamped at −80 mV, and peak I_p was then measured again. Peak I_p after a 5-min washout was also obtained.

Cell shortening measurement. Cell shortening of ventricular myocytes was elicited by field stimulation at 0.5 Hz and was detected by a video edge detector device (Crescent Electronics, Sandy, UT) as previously described (28).

Data and statistics. I_{NCX} and I_p (in pA) were normalized to membrane capacitance (in pF). All data are shown as means ± SE. Student's *t*-test for paired samples was used for statistical analysis unless otherwise indicated.

Mathematical simulation. Simulated *I–V* relationships for I_{NCX} and I_p were based on previous formulations (14). The equation for I_p was as follows:

$$I_p = \bar{I}_p \times f_p \times \frac{1}{1 + \left(\frac{K_{m,Na_i}}{[Na^+]_i}\right)^{1.5}} \times \frac{[K^+]_o}{[K^+]_o + K_{m,K_o}}$$

where $\bar{I}_p$ is maximum I_p, K_{m,Na_i} is the Na^+ half-saturation constant for I_p, $[K^+]_o$ is extracellular K^+ concentration, and K_{m,K_o} is the K^+ half-saturation constant for I_p. The last two terms in the equation describe the pump dependence on $[Na^+]_i$ and $[K^+]_o$. f_p defines the dependence of the pump current on voltage, as follows:

$$f_p = \frac{1}{1 + 0.1245 \times e^{-0.1\frac{VF}{RT}} + 0.0365 \times \sigma \times \exp\left(\frac{-VF}{RT}\right)}$$

where V is voltage, F is Faraday's constant, R is the gas constant, and T is absolute temperature (in K). The factor σ can be further defined as follows:

$$\sigma = \frac{1}{7}\left(e^{\frac{[Na^+]_o}{67.3}} - 1\right)$$

and shows that the voltage dependence can be further modified by extracellular Na^+ concentration ($[Na^+]_o$). In our case, $\bar{I}_p$ is set to 1.88 pA/pF based on the maximum calculated from our own I_p versus $[Na^+]_i$ plot (Fig. 1*D*) instead of 1.5 pA/pF from the publication. All other parameter values were replicated from the original publication or given by experimental conditions: K_{m,Na_i} = 10 mM, K_{m,K_o} = 1.5 mM, $[K^+]_o$ = 5.4 mM, $[Na^+]_o$ = 140 mM, and $[Na^+]_i$ = 10 mM for the basal condition and set at 11.2 mM to simulate effect of 2-meSATP treatment.

I_{NCX} was defined by the following equation:

$$I_{NCX} = k_{NCX} \times \frac{1}{K_{m,Na}^3 + [Na^+]_o^3} \times \frac{1}{K_{m,Ca} + [Ca^{2+}]_o} \times \frac{1}{1 + k_{sat} \times e^{\left[(\eta-1)\frac{VF}{RT}\right]}} \left\{ e^{\left(\eta\frac{VF}{RT}\right)} [Na^+]_i^3 [Ca^{2+}]_o - e^{\left[(\eta-1)\frac{VF}{RT}\right]} [Na^+]_o^3 [Ca^{2+}]_i \right\}$$

where k_{NCX} is a scaling factor of I_{NCX}, $K_{m,Na}$ is the Na^+ half-saturation constant for I_{NCX}, $K_{m,Ca}$ is the Ca^{2+} half-saturation constant for I_{NCX}, k_{sat} is a saturation factor for I_{NCX} at very negative potentials, and η is a factor controlling the voltage dependence of I_{NCX}. $K_{m,Na}$ is 87.5 mM, and $K_{m,Ca}$ is 1.38 mM. Keeping all appropriate concentration values and the original values for k_{sat} and η, an overall scaling factor (k_{NCX}) was estimated to fit our I_{NCX} data using a least-squares fitting method in Excel.

Materials. KB-R7943 and 2-meSATP were obtained from Sigma-Aldrich (St. Louis, MO). YM-244769 was obtained from Tocris Bioscience (Bristol, UK).

RESULTS

Agonist activation of P2X4Rs increased peak I_p. Na^+-K^+-ATPase activity was measured in P2X4R TG ventricular myo-

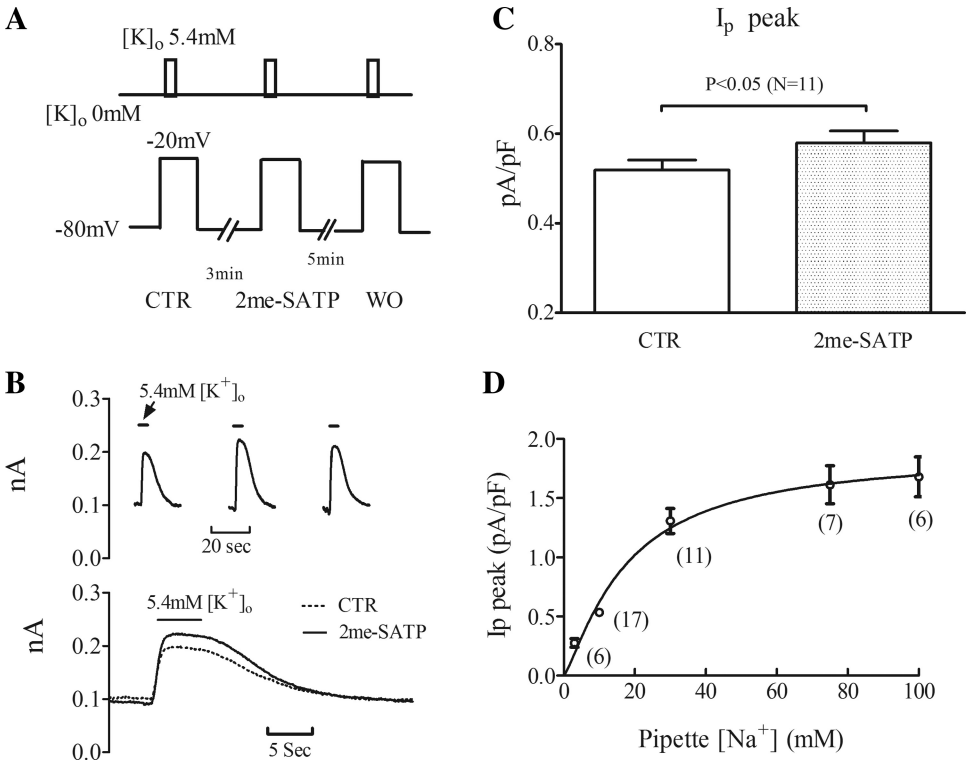

Fig. 1. Peak Na^+-K^+-ATPase current (I_p) increases after 2-methylthio-ATP (2-meSATP) application in P2X4 receptor-overexpressing transgenic (P2X4R TG) cardiac myocytes. *A*, *top*: protocol of the rapid solution changes with 5.4 mM extracellular K^+ concentration ($[K^+]_o$) to elicit K^+-activated I_p. *Bottom*, membrane voltage. I_p was recorded at −20 mV, and 2-meSATP was applied at −80 mV. CTR, control; WO, washout. *B*, *top*: individual traces in a typical myocyte showing the increase of $[K^+]_o$-activated I_p after 2-meSATP application. *Bottom*, superimposed traces of I_p under CTR conditions and with 2-meSATP. *C*: peak I_p, normalized by cell capacitance, is presented as means ± SE. Average CTR peak I_p differed from that with 2-meSATP (n = 11 myocytes from 9 TG mice, $P < 0.05$). *D*: relationship between peak I_p and pipette Na^+ concentration ($[Na^+]$). Peak I_p was elicited by switching $[K^+]_o$ from 0 to 5.4 mM at −20 mV; pipette $[Na^+]$ was varied as shown. Normalized peak I_p is presented as means ± SE. Numbers of cells are indicated in the parentheses (from 18 TG mice).

cytes using the protocol shown in Fig. 1*A*. Thus, 3 μM 2-meSATP induced an inward current (1.4 ± 0.36 pA/pF) in 11 of 17 TG myocytes (from 9 TG mice), confirming our previous results (27). In these myocytes, the effect of the P2X agonist on I_p was determined with a pipette Na^+ concentration of 10 mM (Fig. 1B). In response to 3 μM 2-meSATP, peak I_p increased to 0.58 ± 0.03 pA/pF from a baseline value of 0.52 ± 0.02 pA/pF ($P < 0.05$; Fig. 1*C*), consistent with increased K^+-activated Na^+ pump activity. We next estimated the increase in intracellular Na^+ that could result from the P2X agonist-mediated increase in I_p. To do this, stepwise increments of pipette Na^+ concentration were made and increases in I_p were determined (Fig. 1*D*). The data describing the relationship between pipette Na^+ concentration and I_p were fitted by the following Hill equation: $I = I_{max} \times [Na^+]_p^h/(K_d^h + [Na^+]_p^h)$, where $[Na^+]_p$ is the Na^+ concentration in the pipette and the Hill coefficient (h) was unrestrained and gave a value of 1.25. The K_d value for Na^+ concentration from the equation was 17.6 mM, similar to the value obtained by others (31). Accordingly, back calculating from this equation, the 0.06 ± 0.01 pA/pF net increase in peak I_p would correspond to a 1.08 ± 0.27 mM increase of intracellular Na^+ during P2X agonist application.

P2X agonist enhances the Ca^{2+} entry mode of I_{NCX}. After the baseline Ni^{2+}-sensitive current had been recorded, 3 μM 2-meSATP was applied to myocytes held at −80 mV for 3–4 min. An inward current was observed in 10 of 15 TG myocytes (1.3 ± 0.41 pA/pF from 8 TG mice; Fig. 2*A*), indicating the presence of an inward P2X current. These 10 myocytes were further tested for an effect of the P2X agonist on I_{NCX} by rapidly adding 10 mM $NiCl_2$ to calculate the Ni^{2+}-sensitive current in the presence of 2-meSATP. The data shown in Fig. 2, *B* and *C*, demonstrate that 2-meSATP caused an increase in Ni^{2+}-sensitive current at positive potentials (0.55 ± 0.09 pA/pF under control conditions vs. 0.82 ± 0.14 pA/pF with 2-meSATP at 50 mV, $P < 0.05$). The P2X agonist had a minimal effect on I_{NCX} at negative potentials (−0.46 ± 0.06 pA/pF under control conditions vs. −0.45 ± 0.05 pA/pF with 2-meSATP at −80 mV). These data indicate that 2-meSATP caused an increase of I_{NCX}, notably at its Ca^{2+} entry mode, helping extrude Na^+ in exchange for Ca^{2+}.

From the *I–V* relationships of Ni^{2+} -sensitive currents, the reversal potential of I_{NCX} shifted from −14 ± 2.3 mV under control conditions to −25 ± 4.1 mV in response to 2-meSATP in these myocytes. We next calculated the change of intracellular Na^+ that would cause such a shift of the I_{NCX} reversal potential from the following equations:

$$E_{Na-Ca} = 3 \times E_{Na} - 2 \times E_{Ca}$$

$$E_{Na} = (RT/F) \times \ln[Na^+]_o/[Na^+]_i$$

$$E_{Ca} = (RT/2F) \times \ln[Ca^{2+}]_o/[Ca^{2+}]_i$$

where E_{Na-Ca} is the I_{NCX} reversal potential, E_{Na} is the Na^+ reversal potential, and E_{Ca} is the Ca^{2+} reversal potential, $[Ca^{2+}]_i$ is intracellular Ca^{2+} concentration. In these calculations, the intracellular resting Ca^{2+} was assumed to be 100 nM. With a negative shift of 11 ± 3.52 mV in the reversal potential of I_{NCX} after 2-meSATP, intracellular Na^+ sensed by NCX would need to increase by 1.28 ± 0.42 mM. If the resting Ca^{2+} was 50 nM, the intracellular Na^+ sensed by NCX would still increase by 1.0 ± 0.34 mM. Subsarcolemmal $[Ca^{2+}]_i$ is difficult to estimate even if there is 10 mM EGTA in the pipette solution. This is due to the fact that EGTA is relatively ineffective in buffering Ca^{2+} within 20–100 nm of the pore (38). Under the physiological condition of a living cardiac myocyte, 2-meSATP may cause an increase, even small, of the

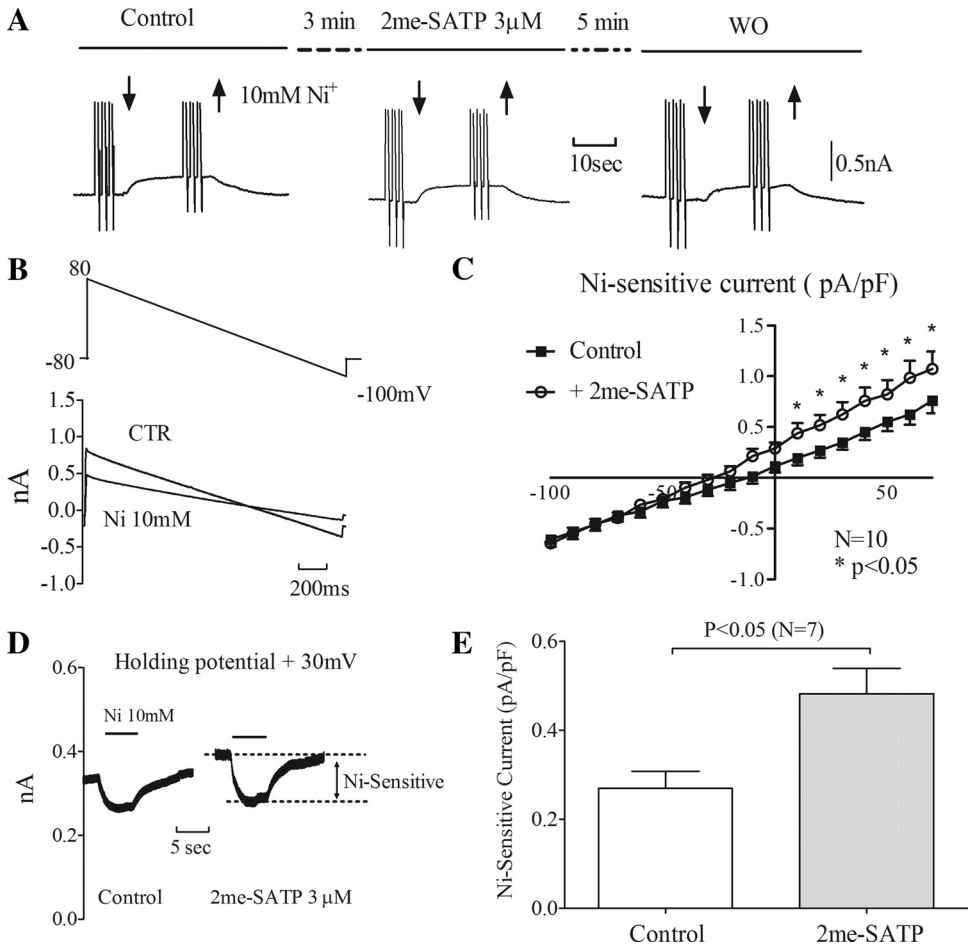

Fig. 2. 2-meSATP increases Na^+/Ca^{2+} exchanger (NCX) current (I_{NCX}). I_{NCX}, represented by Ni^{2+}-sensitive current, in P2X4R TG ventricular myocytes was determined. *A*: representative trace showing membrane current when 10 mM Ni^{2+} was applied (time period bracketed by downward and upward arrows) under CTR conditions, during 2-meSATP application, and after WO. *B*, *top*: descending voltage ramps from 80 to −100 mV were used to contruct the current-voltage (*I–V*) relationship. *Bottom*, typical traces of membrane currents under CTR conditions and in the presence of Ni^{2+}. *C*: mean *I–V* relationships of Ni^{2+}-sensitive current under CTR conditions and in the presence of 2-meSATP. $n = 10$ myocytes from 8 TG mice. $^*P < 0.05$. *D*: 2-meSATP increased the Ca^{2+} entry mode of I_{NCX}. Representative traces are shown for Ni^{2+}-sensitive currents at +30 mV before and after 2-meSATP application in a TG myocyte. *E*: plot of Ni^{2+}-sensitive current at 30 mV under CTR conditions and during 2-meSATP application. $n = 7$ cells from 5 TG mice. $P < 0.05$.

intracellular Ca^{2+} level via direct Ca^{2+} entry through the P2X4R. Under this circumstance, the 1.28 ± 0.42-mM increase of Na^+ in the subsarcolemmal space might be an underestimate. Overall, while we could not be certain of the exact subsarcolemmal Ca^{2+} level, whatever the presumed level of Ca^{2+}, $[Na^+]_i$ would have to increase to cause the observed shift of NCX reversal potential.

To verify that 2-meSATP increases the Ca^{2+} entry mode of I_{NCX}, Ni^{2+}-sensitive current was measured at a holding potential of +30 mV without running the ramp protocol before and after 3 μM 2-meSATP application (Fig. 2*D*). At 30 mV, Ni^{2+}-sensitive current increased from 0.28 ± 0.04 pA/pF under control conditions to 0.48 ± 0.06 pA/pF ($P < 0.05$) after 2-meSATP (Fig. 2*E*). Thus, by either voltage ramp or step, the P2X agonist elicited an increase in the Ca^{2+} entry mode of I_{NCX}.

Simulated I-V relationships. The experimental data indicate that elevation of $[Na^+]_i$ by P2X4R activation results in an increase of I_p and I_{NCX}. We asked whether a simulated rise in $[Na^+]_i$ of the same magnitude can cause an increase of I_p and I_{NCX} like that observed experimentally in P2X4R-overexpressing TG myocytes. Computationally (see MATERIALS AND METHODS), when cellular Na^+ was increased by 1.2 mM, a magnitude similar to that estimated by the experimentally measured stimulation of I_{NCX} or I_p by 2-meSATP, the computationally predicted *I–V* relationship of I_p closely matched the experimentally observed increase in I_p (Fig. 3*A*). Similarly, the computationally derived *I–V* relationship of I_{NCX} agreed well with our experimental results (Fig. 3*B*). Thus, based on established mathematical models for the NCX and the Na^+ pump (14), the increase in $[Na^+]_i$ and its corresponding stimulation of I_{NCX} and I_p agreed well with our experimental results.

We modified the scaling factor from 1.5 pA/pF in the original equation for the I_p model (14) to our experimentally measured $\bar{I}_p$ at 1.88 pA/pF. In the computerized model, I_p is outwardly directed over the entire test potential range (−80 to +50 mV) and is increased after a 1.2-mM increment of intracellular Na^+ (Fig. 3*A*). At −20 mV, the predicted increase in I_p (0.04 pA/pF) was similar to the experimentally determined increase of 0.06 ± 0.01 pA/pF after stimulation by 2-meSATP.

In the modeling of I_{NCX}, the best fit for our experimental I_{NCX} data caused us to use a k_{NCX} value of 2,606.64 pA/pF instead of 2,000 pA/pF, as used by others (14). The modeled *I–V* relationship of NCX shifted leftward upon the 1.2-mM step increase of intracellular Na^+ from 10 to 11.2 mM. This leftward shift was not a parallel change since the primary effect was an increase in the Ca^{2+} entry mode of I_{NCX} with little if any change in the Ca^{2+} exit mode. The computed shift of the *I–V* curve for I_{NCX} was similar to the experimentally observed shift by 2-meSATP (Fig. 3*B*). At +50 mV, the modeled Ca^{2+} entry mode increased from 0.60 pA/pF at 10 mM $[Na^+]_i$ to 0.86 pA/pF at 11.2mM $[Na^+]_i$ (net increase of 0.26 pA/pF). This modeled increase agreed well with that observed experi-

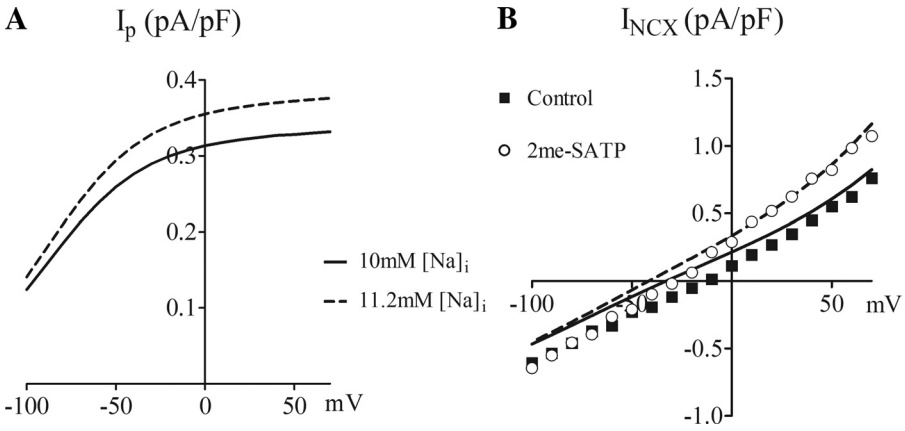

Fig. 3. Simulated *I–V* relationships with 10 and 11.2 mM intracellular $[Na^+]$ ($[Na^+]_i$). *A*: simulation of I_p with $[Na^+]_i$ taken as cellular (pipette) $[Na^+]$ of 10 and 11.2 mM. *B*: simulation of I_{NCX} with intracellular Ca^{2+} concentration kept constant at 100 nM for cellular $[Na^+]$ of 10 and 11.2 mM. The actual experimental data under CTR conditions and after 2-meSATP application were also plotted for comparison with the simulation.

mentally (net increase of 0.27 ± 0.10 pA/pF; Fig. 2*C*). Overall, an elevated intracellular Na^+ level has a more detectable effect on the Ca^{2+} entry mode rather than the Ca^{2+} exit mode of I_{NCX}.

KB-R7943 or YM-244769 inhibits the 2-meSATP-induced increase of cell shortening. Extracellular 2-meSATP increases cell shortening in TG cardiac myocytes (27). To explore if the Ca^{2+} entry mode of I_{NCX} contributes to the increase of cell shortening by 2-meSATP in TG cardiac myocytes, KB-R7943 and a structurally different NCX inhibitor, YM-244769 (10), both of which preferentially oppose the Ca^{2+} entry mode, were tested in TG myocytes. KB-R7943 at 5 μM or YM-244769 at 0.1 μM did not alter the basal cell shortening of TG myocytes (total of 19 myocytes from 7 TG mice; Fig. 4*B*). Superfusion with 3 μM 2-meSATP increased cell shortening by 29.2 ± 3.7% above basal in 16 of 23 TG cardiac myocytes (from 10 TG mice) paced at 0.5 Hz ($P < 0.05$). When 5 μM KB-R7943 was added in the continued presence of 2-meSATP, the increase of cell shortening was reduced to 13.8 ± 3.9% above basal ($P < 0.05$; Fig. 4, *A* and *C*). In another set of similar experiments, we tested the effect on 2-meSATP-stimulated cell shortening by YM-244769. In these experiments, 3 μM 2-meSATP increased cell shortening by 31.4 ± 7.1% in 10 of 15 TG cardiac myocytes (from 6 TG mice) paced at 0.5 Hz ($P < 0.05$). At 0.1 μM, YM-244769 reduced 3 μM 2-meSATP-stimulated cell shortening to 17.3 ± 7.4% above basal ($P < 0.05$; Fig. 4*D*). Thus, either KB-R7943 or YM-244769 could inhibit the 2-meSATP-induced increase of cell shortening, indicating a role of the Ca^{2+} entry mode in mediating the P2X agonist effect on myocyte contractility in these TG myocytes.

P2X agonist can stimulate I_{NCX} in WT ventricular myocytes. To explore the physiological relevance of this receptor in modulating Na^+ handling, the effects of a P2X agonist on I_{NCX}

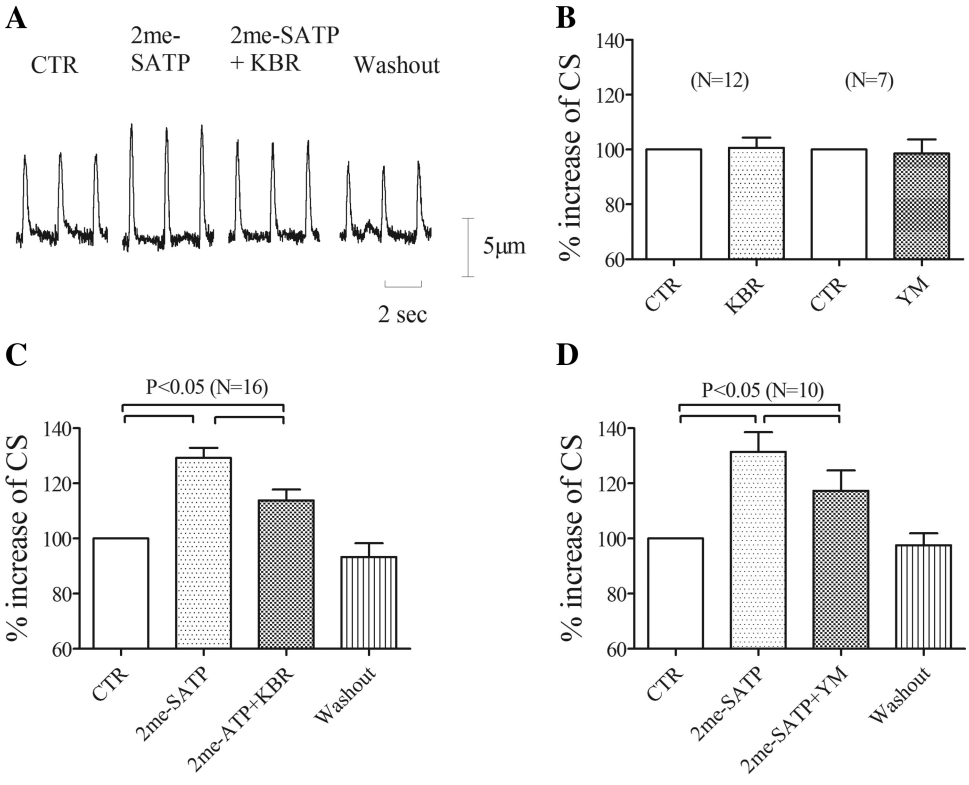

Fig. 4. KB-R7943 (KBR) or YM-244769 (YM) inhibits the 2-meSATP-induced increase of cell shortening (CS). *A*: representative traces of CS in TG myocytes paced at 0.5 Hz for cells exposed to 2-meSATP and then to 2-meSATP plus KBR followed by WO. *B*: basal CS did not change after application of KBR ($n = 12$) or YM ($n = 7$). *C*: percent increases of CS above basal during application of 2-meSATP alone (percent above basal, $n = 16$ cells from 10 Tg mice) and during the addition of KBR plus 2-meSATP (percent above basal with both KBR and 2-meSATP vs. that with 2-meSATP alone, $P < 0.05$). *D*: percent increases of CS above basal during application of 2-meSATP alone (percent above basal, $n = 10$ cells from 6 Tg mice) and during exposure of YM plus 2-meSATP (percent above basal with both YM and 2-meSATP vs. that with 2-meSATP alone, $P < 0.05$).

and myocyte contraction were tested in cardiac ventricular myocytes of WT mice. Application of 10 μM 2-meSATP induced an inward current at −80 mV (0.68 ± 0.26 pA/pF) in 8 of 34 WT ventricular myocytes (from 7 WT mice), similar to our previous findings (27). These P2X agonist-responsive myocytes were then tested for changes in I_{NCX}. 2-meSATP increased Ni^{2+}-sensitive current at positive potentials (0.46 ± 0.05 pA/pF at baseline vs. 0.59 ± 0.06 pA/pF with 2-meSATP at +50 mV, $P < 0.05$; Fig. 5*A*). There were no significant changes by 2-meSATP in Ni^{2+}-sensitive current at negative potentials (−0.40 ± 0.09 pA/pF under control conditions vs. −0.42 ± 0.09 pA/pF with agonist at −80 mV, $P > 0.05$). The primary effect on the Ca^{2+} entry mode but not the Ca^{2+} exit mode of NCX in WT myocytes was qualitatively the same as that found in myocytes from P2X4 TG hearts. The reversal potential of I_{NCX} shifted from −13.25 ± 1.72 to −17.5 ± 1.29 mV in response to 2-meSATP ($P < 0.05$). These data demonstrate that a P2X agonist can also elicit an increase in the Ca^{2+} entry mode of NCX in WT myocytes.

As further evidence for a physiological role of cardiac P2X4Rs, the effect of KB-R7943 on the P2X agonist-induced increase of cell shortening was tested in WT murine cardiac myocytes. In WT myocytes, the P2X agonist had little or no effect on basal contraction. To facilitate detection of an agonist-stimulated effect on cell shortening in WT myocytes, 3 μM ivermectin, which selectively potentiates the P2X4 effect (17), was combined with 10 μM 2-meSATP. The combined presence of 2-meSATP and ivermectin increased cell shortening by 14.8 ± 3.1% above basal in 8 of 32 WT myocytes (from 7 WT mice) paced at 0.5 Hz ($P < 0.05$). The addition of 5 μM KB-R7943 to 2-meSATP plus ivermectin reduced cell shortening to 7.2 ± 2.3% above basal ($P < 0.05$; Fig. 5*B*), similar to the response elicited by KB-R7943 in TG myocytes. The data support a link between the Ca^{2+} entry mode of NCX and P2X4Rs in WT myocytes.

DISCUSSION

P2XRs are a family of ligand-gated ion channels (17, 36). P2X4Rs are an important subtype of the endogenous P2XR channel in the cardiac myocyte. When activated by extracellular ATP, these channels conduct cations in a voltage-dependent manner with a reversal potential near 0 mV (17, 22). As a Na^+ entry pathway, these channels may have a physiological role in regulating cellular Na^+ levels in cardiac myocytes. The objective here was to test the hypothesis that activation of these channels by extracellular ATP causes an increased cellular Na^+ level in cardiac myocytes. We further determined whether the P2XR-induced stimulation of NCX has a role in modulating the contractile state of cardiac myocytes.

In the present study, we used myocytes from both TG and WT mice to test these concepts, which are supported by the following lines of evidence. First, the P2XR-mediated increase in Na^+ entry into the myocyte (27) should stimulate I_p because the pump functions to extrude intracellular Na^+. Indeed, activation of the P2X4R by its agonist, 2-meSATP, was able to increase I_p in TG cardiac myocytes. Second, P2X agonist should stimulate I_{NCX}, another cellular mechanism for Na^+ extrusion. We found that in both WT and TG cardiac myocytes, 2-meSATP could stimulate the Ca^{2+} entry mode of NCX. Third, an increase in cellular $[Na^+]_i$ due to P2XR-mediated Na^+ entry can be estimated in TG myocytes. For I_p, which was only measured in TG myocytes, the magnitude of $[Na^+]_i$ increase (1.08 ± 0.27 mM) was calculated based on responses calibrated to concentration changes in pipette and, hence, cytosolic Na^+. For I_{NCX}, the receptor-mediated shift of reversal potential yielded a Na^+ increase of 1.28 ± 0.42 mM, assuming constant intracellular Ca^{2+}. These data provided experimental evidence under voltage-clamp conditions that stimulation of P2XRs can result in measurable cellular Na^+ increases. Fourth, computational modeling, assuming an increment of $[Na^+]_i$ like that observed experimentally, replicated the experimental findings and permitted estimation of the pattern and magnitude of increases in I_p and I_{NCX}. The simulated effects on I_p and I_{NCX} from the increase in $[Na^+]_i$ were similar to previously established dependencies of these currents on ionic concentrations and voltage. Experimentally, activation of the P2X4 channel primarily increases the Ca^{2+} entry mode of NCX. Computationally simulated *I–V* relationships of I_{NCX} in response to a similarly increased cellular Na^+ concentration also showed an increase in only the Ca^{2+} entry mode. There was minimal effect on the Ca^{2+} exit mode of NCX in the simulation. Overall, the computer simulation agreed with experimental data regarding the cellular ionic effects on I_p and I_{NCX}. P2X agonist also induced a similar pattern of increase of the Ca^{2+} entry mode of NCX in cardiac ventricular myocytes from WT animals, supporting a physiological role of the cardiac P2XR in the regulation of Na^+ handling.

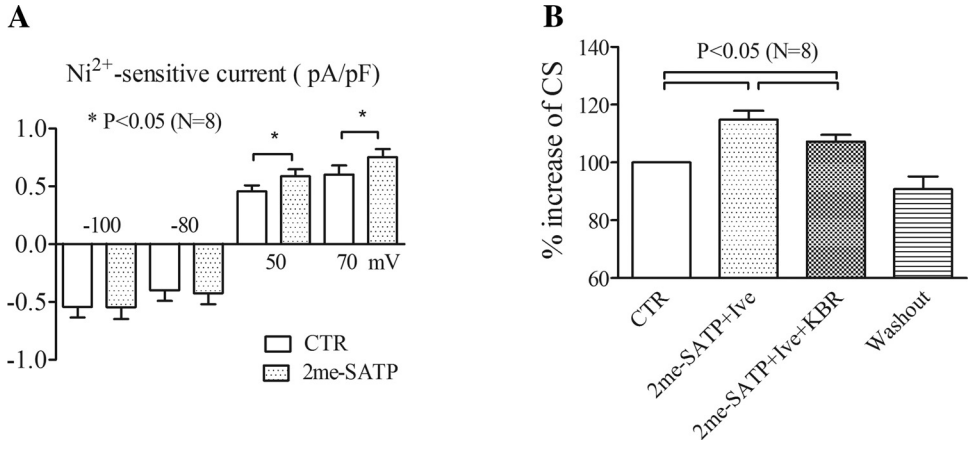

Fig. 5. Link between P2X receptors and NCX in wild-type (WT) myocytes. *A*: 2-meSATP-induced increase of I_{NCX} in WT myocytes. Ni^{2+}-sensitive currents before and after 2-meSATP application are shown at membrane potentials of −100, −80, 50, and 70 mV. I_{NCX} at +50 and +70 mV was significantly larger in the presence of 2-meSATP than under CTR conditions ($n = 8$ cells from 7 WT mice). *$P < 0.05$. *B*: percent increases of CS above basal during application of 2-meSATP plus ivermectin (Ive; percent above basal, $n = 8$ cells from 7 WT mice) and during the subsequent exposure of KBR plus 2-meSATP and Ive (percent above basal with KBR plus 2-meSATP and Ive vs. that with 2-meSATP plus Ive, $P < 0.05$).

We attempted to measure directly $[Na^+]_i$ in TG myocytes using the fluorescent Na^+ indicator sodium benzofuran isophtalate. We could not detect any change in $[Na^+]_i$ after 2-meSATP application in P2X4R TG myocytes (data not shown). This is not surprising given that the amount of the cellular Na^+ increase is below the sensitivity of this Na^+-sensitive dye, the K_d of which is 3.8 mM in the absence of K^+ and 11.3 mM in the presence of physiological concentrations of K^+ (Molecular Probes website). Swift et al. (32) observed that a low concentration of ouabain (0.3 μM) increased contractility by 40% via its selective inhibition of the α_2-isoform of the Na^+ pump, but they could not detect an increase in global $[Na^+]_i$ by sodium benzofuran isophtalate in rat cardiac myocytes. They concluded that the increased contractility in response to 0.3 μM ouabain could not be explained by a substantial global rise in $[Na^+]_i$. Similar to our finding of a P2X agonist-induced stimulation of NCX, a local accumulation of $[Na^+]_i$ after ouabain was detectable by I_{NCX} measurements (32). It is thought that the Na^+ concentration in the subsarcolemmal space is sensed by the Na^+ pump, NCX, and other membrane transport mechanisms (3, 12, 13). It is possible that the increase in I_{NCX} or I_p measured during cardiac P2X4 activation reflects an increase in subsarcolemmal Na^+ concentrations.

In studying the role of NCX in mediating the P2XR-induced effect on contraction, we used P2X4R-overexpressing TG cardiac myocytes. TG myocytes displayed a greater magnitude of P2XR-mediated increase in contraction and were a better model to determine the mechanism of the contractile effect of P2X agonist. We postulated that the Ca^{2+} entry mode of NCX, stimulated by an intracellular Na^+ elevation, contributes to the contraction increase by P2X agonist. This postulate is supported by our finding that the P2X agonist was able to enhance sarcoplasmic reticulum Ca^{2+} content in P2X4R TG myocytes (29). In the present study, KB-R7943 could inhibit the 2-meSATP-induced increase in cell shortening in TG myocytes. KB-R7943, at 5 μM, can serve as a selective Ca^{2+} entry mode inhibitor (23, 24). Another structurally different selective inhibitor of the Ca^{2+} entry mode (10), YM-244769, was also able to inhibit the 2-meSATP-induced stimulation of cell shortening in TG cells. Neither KB-R7943 nor YM-244769 affected basal cell shortening in these cardiac myocytes.

Several considerations deserve to be mentioned. Ca^{2+} may enter directly through the P2X4R. Ca^{2+} could contribute as much as 8% of the total inward current induced by ATP via the human homotrimeric P2X4R (4). Direct Ca^{2+} entry via the P2XR may dynamically impact cellular Na^+ by further increasing the accumulation of Na^+ that enters through the receptor under physiological condition in myocytes. We could not exclude that P2X agonist increases subsarcolemmal $[Ca^{2+}]_i$ via direct Ca^{2+} entry through the receptor channel. A direct measurement of subsarcolemmal $[Ca^{2+}]_i$ during P2X agonist stimulation was not feasible in the present study.

Another implication of P2XR activation merits further consideration. That both I_{NCX} and I_p can extrude P2XR-mediated Na^+ entry distinguishes the P2X effect from the contractile and proarrhythmic effects of digitalis. Digitalis, by inhibiting Na^+-K^+-ATPase and thus causing an increase in intracellular Na^+, results in NCX as the only Na^+-extruding mechanism in digitalis-treated cardiac myocytes. Since both I_{NCX} and I_p can operate to extrude P2XR-conducted Na^+ entry, the cell is less likely to be overloaded by intracellular Na^+ and Ca^{2+} during stimulation of P2XRs. The physiological relevance of cardiac myocyte P2XRs is supported by the demonstration in WT cardiac myocytes that P2X agonist can stimulate NCX. Endogenous cardiac P2X4Rs in WT cardiac myocytes, when enhanced by ivermectin, could modulate the contractile state, supporting a link between NCX and P2X4Rs. That only a fraction of the WT myocytes studied had a response may be explained by one or more reasons. As these cell surface P2XRs are susceptible to degradation by proteases during the enzymatic isolation procedure (27), it is possible that only some of the WT myocytes retained functional cell surface expression. As acutely dispersed cardiac myocytes, some may show more internalization than others. There is recent evidence for internalization of these cell surface P2X4Rs into early endosomes (21). It is possible that the isolation procedure could have induced more internalization. Overall, we interpret the result as indicating that WT myocytes are capable of mounting either contractile or I_{NCX} response to P2X agonist.

A further question relates to the significance of the ~1-mM increase in $[Na^+]_i$ induced by P2X4Rs in TG myocytes. In ouabain-treated Purkinje fibers, a 1-mM rise of $[Na^+]_i$ induced a doubling of contractile force in Purkinje fibers, although a similar increase in $[Na^+]_i$ caused a less robust increase in contractile function in ventricular muscle (2). Thus, a small increase of $[Na^+]_i$ could have a significant impact on cardiac contractile function. In the present study, the cardiac P2XR-induced increase in $[Na^+]_i$ was obtained when NCX or the Na^+ pump was blocked. In a living cardiac myocyte, Na^+ entry via P2XRs could exit the cell via both NCX and the Na^+ pump. Actual dynamic submembrane Na^+ may be <1.0 mM but may be sufficient to cause an increase in microdomain Ca^{2+} via the Ca^{2+} entry mode of NCX near or at the endothelial nitric oxide synthase (eNOS) enzyme.

Cardiac P2X4Rs may also be implicated under pathophysiological condition. mRNAs encoding all of the P2XRs have been demonstrated in the human left ventricle. P2XR protein expression was confirmed for all P2XRs except for P2X5 (1). In left ventricular tissue from patients with congestive heart failure, the expression for P2X6 was upregulated compared with healthy control subjects (1). Healthy tissues from the human right atrium and sinoatrial node also express P2X4, P2X5, P2X6, and P2X7 receptors, with P2X4Rs and P2X7 receptors being the most abundant (16). Although these data do not localize the level of expression of P2X4Rs on endothelial cells, fibroblasts, or cardiac myocytes in the intact heart, it is likely that P2X4Rs on human cardiac myocytes have a role in regulating cardiac function under pathophysiological conditions such as heart failure or hypertrophy. Animal studies have lended further support to this concept. Calsequestrin-overexpressing cardiomyopathic hearts show an upregulation of P2X4Rs by immunoblot analysis and increased P2X current by 2-meSATP compared with WT hearts (26). More recently, it has been shown that hypoxia could stimulate P2X4R upregulation in the right ventricle of rats (18). Upregulated cardiac P2X4Rs during heart failure or hypoxia may exert a greater Na^+ handling effect under such pathological conditions. Whether upregulation represents a compensatory salutary effect or causes the progression of heart disease remains to be determined. It is of interest that cardiac P2X4R overexpression has a salutary effect in heart failure and that knockout of endogenous cardiac myocyte P2X4Rs results in a more severe

heart failure phenotype (37). The mechanism of cardioprotection was shown to be activation of eNOS, presumably due to a localized microdomain Ca^{2+} increase, which was, in turn, from the increased Ca^{2+} entry mode of NCX and direct Ca^{2+} conductance via the P2X4 channel. The data imply that any upregulation of P2X4Rs during heart failure is a compensatory protective mechanism.

In conclusion, the present study demonstrated a novel Na^+ entry pathway through a sarcolemmal ligand-gated ion channel in adult murine ventricular myocytes of both receptor-overexpressing TG and WT mice. Both the experimental and simulated data on Na^+-K^+-ATPase and NCX highlighted a new Na^+ entry pathway via the myocyte P2XR. Given the recent finding that cardiac P2X4Rs physically associate with eNOS (37), this purinergic Na^+ entry pathway likely has important implications in the regulation of cardiac function.

ACKNOWLEDGMENTS

The authors thank Dr. Leslie Loew (Center for Cell Analysis and Modeling, University of Connecticut) for the advice on mathematical simulation of currents and Carol McGuiness for the expert care of the study animals.

GRANTS

The work was supported by the Pat and Jim Calhoun Cardiology Research Fund and in part by National Heart, Lung, and Blood Institute Grant HL-48225.

DISCLOSURES

No conflicts of interest, financial or otherwise, are declared by the author(s).

AUTHOR CONTRIBUTIONS

Author contributions: J.-B.S. and R.Y. performed experiments; J.-B.S., R.Y., A.J.P., and B.T.L. analyzed data; J.-B.S. and R.Y. prepared figures; J.-B.S. and R.Y. drafted manuscript; J.-B.S., R.Y., A.J.P., and B.T.L. approved final version of manuscript; R.Y., A.J.P., and B.T.L. interpreted results of experiments; A.J.P. and B.T.L. conception and design of research; A.J.P. and B.T.L. edited and revised manuscript.

REFERENCES

1. **Banfi C, Ferrario S, De Vincenti O, Ceruti S, Fumagalli M, Mazzola A, D'Ambrosi N, Volonte C, Fratto P, Vitali E, Burnstock G, Beltrami E, Parolari A, Polvani G, Biglioli P, Tremoli E, Abbracchio MP.** P2 receptors in human heart: upregulation of P2X6 in patients undergoing heart transplantation, interaction with TNFα and potential role in myocardial cell death. *J Mol Cell Cardiol* 39: 929–939, 2005.
2. **Bers D.** *Excitation-Contraction Coupling and Cardiac Contractile Force (Developments in Cardiovascular Medicine)*. Dordrecht: Springer, 2008.
3. **Carmeliet E.** A fuzzy subsarcolemmal space for intracellular Na^+ in cardiac cells? *Cardiovasc Res* 26: 433–442, 1992.
4. **Garcia-Guzman M, Soto F, Gomez-Hernandez JM, Lund PE, Stuhmer W.** Characterization of recombinant human P2X4 receptor reveals pharmacological differences to the rat homologue. *Mol Pharmacol* 51: 109–118, 1997.
5. **Ginsberg KS, Bers DM.** Isoproterenol does not enhance Ca-dependent Na/Ca exchange current in intact rabbit ventricular myocytes. *J Mol Cell Cardiol* 39: 972–981, 2005.
6. **Glitsch HG.** Electrophysiology of the sodium-potassium-ATPase in cardiac cells. *Physiol Rev* 81: 1791–1826, 2001.
7. **Hinata M, Kimura J.** Forefront of Na^+/Ca^{2+} exchanger studies: stoichiometry of cardiac Na^+/Ca^{2+} exchanger; 3:1 or 4:1? *J Pharmacol Sci* 96: 15–18, 2004.
8. **Hu B, Mei QB, Yao XJ, Smith E, Barry WH, Liang BT.** A novel contractile phenotype with cardiac transgenic expression of the human P2X4 receptor. *FASEB J* 15: 2739–2741, 2001.
9. **Hu B, Senkler C, Yang A, Soto F, Liang BT.** P2X4 receptor is a glycosylated cardiac receptor mediating a positive inotropic response to ATP. *J Biol Chem* 277: 15752–15757, 2002.
10. **Iwamoto T, Kita S.** YM-244769, a novel Na^+/Ca^{2+} exchanger inhibitor that preferentially inhibits NCX3, efficiently protects against hypoxia/reoxygenation-induced SH-SY5Y neuronal cell damage. *Mol Pharmacol* 70: 2075–2083, 2006.
11. **Kimura J, Miyamae S, Noma A.** Identification of sodium-calcium exchange current in single ventricular cells of guinea-pig. *J Physiol* 384: 199–222, 1987.
12. **Lederer WJ, Niggli E, Hadley RW.** Sodium-calcium exchange in excitable cells: fuzzy space. *Science* 248: 283, 1990.
13. **Levi AJ, Boyett MR, Lee CO.** The cellular actions of digitalis glycosides on the heart. *Prog Biophys Mol Biol* 62: 1–54, 1994.
14. **Luo CH, Rudy Y.** A dynamic model of the cardiac ventricular action potential. I. Simulations of ionic currents and concentration changes. *Circ Res* 74: 1071–1096, 1994.
15. **Mei Q, Liang BT.** P2 purinergic receptor activation enhances cardiac contractility in isolated rat and mouse hearts. *Am J Physiol Heart Circ Physiol* 281: H334–H341, 2001.
16. **Musa H, Tellez JO, Chandler NJ, Greener ID, Maczewski M, Mackiewicz U, Beresewicz A, Molenaar P, Boyett MR, Dobrzynski H.** P2 purinergic receptor mRNA in rat and human sinoatrial node and other heart regions. *Naunyn Schmiedebergs Arch Pharmacol* 379: 541–549, 2009.
17. **North RA.** Molecular physiology of P2X receptors. *Physiol Rev* 82: 1013–1067, 2002.
18. **Ohata Y, Ogata S, Nakanishi K, Kanazawa F, Uenoyama M, Hiroi S, Tominaga S, Kawai T.** Expression og P2X4R mRNA and protein in rats with hypobaric hypoxia-induced pulmonary hypertension. *Circ J* 75: 945–954, 2011.
19. **Parker KE, Scarpa A.** An ATP-activated nonselective cation channel in guinea pig ventricular myocytes. *Am J Physiol Heart Circ Physiol* 269: H789–H797, 1995.
20. **Podrasky E, Xu D, Liang BT.** A novel phospholipase C- and cAMP-independent positive inotropic mechanism via a P2 purinoceptor. *Am J Physiol Heart Circ Physiol* 273: H2380–H2387, 1997.
21. **Qureshi OS, Paramasivam A, Yu JC, Murrell-Lagnado RD.** Regulation of $P2X_4$ receptors by lysosomal targeting, glycan protection and exocytosis. *J Cell Sci* 120: 3838–3749, 2007.
22. **Ralevic V, Burnstock G.** Receptors for purines and pyrimidines. *Pharmacol Rev* 50: 413–492, 1998.
23. **Satoh H, Ginsburg KS, Qing K, Terada H, Hayashi H, Bers DM.** KB-R7943 block of Ca^{2+} influx via Na^+/Ca^{2+} exchange does not alter twitches or glycoside inotropy but prevents Ca^{2+} overload in rat ventricular myocytes. *Circulation* 101: 1441–1446, 2000.
24. **Satoh H, Mukai M, Urushida T, Katoh H, Terada H, Hayashi H.** Importance of Ca^{2+} influx by Na^+/Ca^{2+} exchange under normal and sodium-loaded conditions in mammalian ventricles. *Mol Cell Biochem* 242: 11–17, 2003.
25. **Scamps F, Vassort G.** Pharmacological profile of the ATP-mediated increase in L-type calcium current amplitude and activation of a non-specific cationic current in rat ventricular cells. *Br J Pharmacol* 113: 982–986, 1994.
26. **Shen JB, Cronin C, Sonin D, Joshi BV, Nieto MG, Harrison D, Jacobson KA, Liang BT.** P2X purinergic receptor-mediated ionic current in cardiac myocytes of calsequestrin model of cardiomyopathy: implications for the treatment of heart failure. *Am J Physiol Heart Circ Physiol* 292: H1077–H1084, 2007.
27. **Shen JB, Pappano AJ, Liang BT.** Extracellular ATP-stimulated current in wild-type and P2X4 receptor transgenic mouse ventricular myocytes: implications for a cardiac physiologic role of P2X4 receptors. *FASEB J* 20: 277–284, 2006.
28. **Shen JB, Shutt R, Agosto M, Pappano A, Liang BT.** Reversal of cardiac myocyte dysfunction as a unique mechanism of rescue by P2X4 receptors in cardiomyopathy. *Am J Physiol Heart Circ Physiol* 296: H1089–H1095, 2009.
29. **Shen JB, Shutt R, Pappano A, Liang BT.** Characterization and mechanism of P2X receptor-mediated increase in cardiac myocyte contractility. *Am J Physiol Heart Circ Physiol* 293: H3056–H3062, 2007.
30. **Sonin D, Zhou SY, Cronin C, Sonina T, Wu J, Jacobson KA, Pappano A, Liang BT.** Role of P2X purinergic receptors in the rescue of ischemic heart failure. *Am J Physiol Heart Circ Physiol* 295: H1191–H1197, 2008.
31. **Su Z, Zou A, Nonaka A, Zubair I, Sanguinetti MC, Barry WH.** Influence of prior Na^+ pump activity on pump and Na^+/Ca^{2+} exchange currents in mouse ventricular myocytes. *Am J Physiol Heart Circ Physiol* 275: H1808–H1817, 1998.

32. **Swift F, Tovsrud N, Enger UH, Sjaastad I, Sejersted OM.** The Na^+/K^+-ATPase α2-isoform regulates cardiac contractility in rat cardiomyocytes. *Cardiovasc Res* 75: 109–117, 2007.
33. **Verdonck F, Volders PG, Vos MA, Sipido KR.** Intracellular Na^+ and altered Na^+ transport mechanisms in cardiac hypertrophy and failure. *J Mol Cell Cardiol* 35: 5–25, 2003.
34. **Wang W, Gao J, Entcheva E, Cohen IS, Gordon C, Mathias RT.** A transmural gradient in the cardiac Na/K pump generates a transmural gradient in Na/Ca exchange. *J Membr Biol* 233: 51–62, 2010.
35. **Yang A, Sonin D, Jones L, Barry WH, Liang BT.** A beneficial role of cardiac P2X4 receptors in heart failure: rescue of the calsequestrin overexpression model of cardiomyopathy. *Am J Physiol Heart Circ Physiol* 287: H1096–H1103, 2004.
36. **Yang R, Liang BT.** Cardiac P2X4 receptors: targets in ischemia and heart failure? *Circ Res* 111: 397–401, 2012.
37. **Yang T, Shen JB, Yang R, Redden J, Dodge-Kafka K, Grady J, Jacobson KA, Liang BT.** Novel protective role of endogenous cardiac myocyte P2X4 receptors in heart failure. *Circ Heart Fail* 7: 510–518, 2014.
38. **You Y, Pelzer DJ, Pelzer S.** Modulation of L-type Ca^{2+} current by fast and slow Ca^{2+} buffering in guinea pig ventricular cardiomyocytes. *Biophys J* 72: 175–187, 1997.